Effects of refraction on tomographic reconstruction

Tony Hyun Kim[1,*]

[1] *Department of Electrical Engineering, Stanford University, Stanford, CA 94305*

compiled: March 17, 2013

In practical implementations of tomographic systems, wave phenomena such as refraction represent deviations from the idealized case of straight line tomography. In this paper, a commercial optical design software (Zemax) is used to compute numerically accurate projection integrals along refracted ray paths given arbitrary source distributions. These "refraction projections" are then fed as inputs to a standard ρ-filter backprojection algorithm, and the effect of refraction on the reconstructed distributions is visualized.

1. Introduction

The basic mathematical problem of tomography is to reconstruct a two-dimensional "source" function $f(x, y)$ given a set of one-dimensional line integrals of f. In such an idealized tomography set-up, the projections can be construed as a representation of f in the basis of line delta functions, and an elegant mathematical principle – the Projection-Slice Theorem – shows that a perfect reconstruction of f can be performed.

In practice, the various implementations of tomographic measurement and reconstruction violate the straight line integral assumption of the mathematical problem. For instance, in electromagnetic (radio, microwave, optical) or ultrasound tomography set-ups, the line integral measurement is understood to be along the ray direction, which will refract or even undergo complicated reflections within the sample. In such cases, the path integral will be perturbed from the idealized straight line, where the exact perturbation will be object (*i.e.* $f(x, y)$) dependent.

In this paper, we regard refraction as a perturbation to the straight line tomography and evaluate its effects. A novel feature of the current work is the integration of a commercial optical design software Zemax (Radiant Zemax LLC) whose ray tracing engine is used for accurate refracted path calculations. (Particularly interesting is Zemax's ability to import arbitrarily complex CAD models of potential tomography targets.) The numerical experiment will be as follows: first, we develop the filtered backprojection algorithm for reconstructing $f(x, y)$ assuming straight line integrals; second, we set up the refracted path forward model in Zemax; finally, we use the refracted path projections as the input to the backprojection algorithm, and compare the results to the actual source distribution.

This work is part of an ongoing fascination with the elegant mathematical problem of tomographic reconstruction. Given that in practice, physical complications such as refraction are always present, it is of great personal interest to understand how the complications theoretically affect the tomography problem and to discover high-performing and/or efficient algorithms for their correction or even take advantage of the additional physics.

2. Basic set-up

In this section, we describe the set-up of the numerical "refracted tomography" experiment, in which we feed refracted path length projections as inputs to the filtered-backprojection reconstruction algorithm.

2.A. Tomography geometry

Since we are performing numerical experiments, it is not absolutely necessary to give explicit physical dimen-

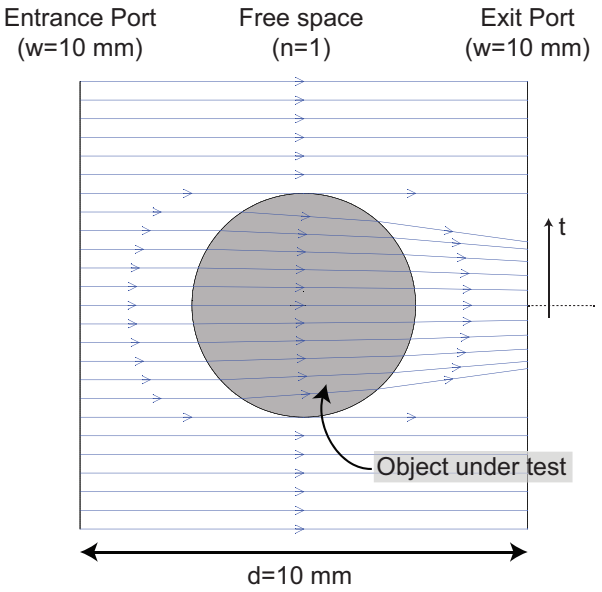

Fig. 1. Basic dimensions of the numerical tomography setup. The entire workspace is 10 mm × 10 mm. Arbitrary objects can be inserted at any position into the workspace. The transverse intercept of a ray at the exit port is given by t.

* kimth@stanford.edu

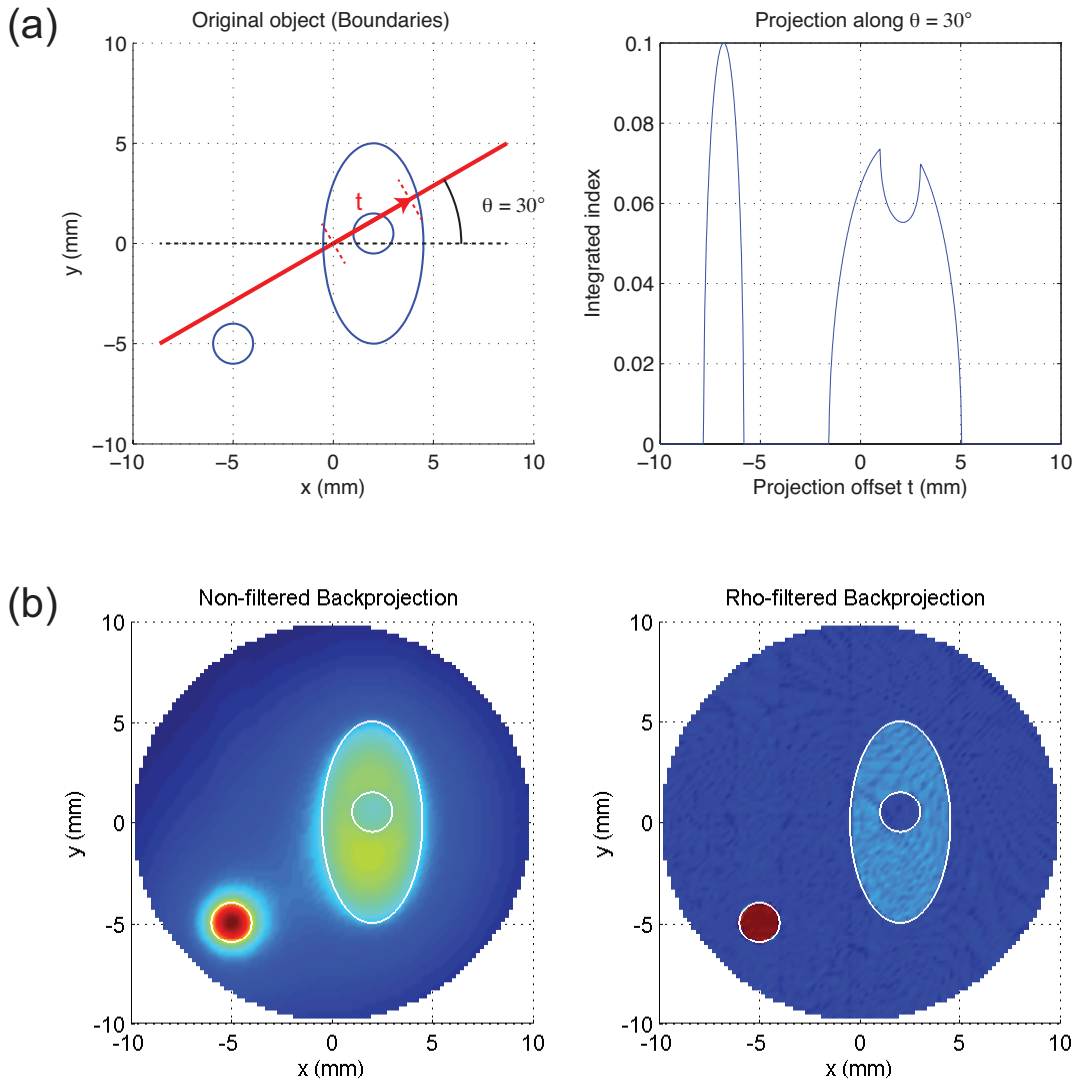

Fig. 2. Demonstration of the standard filtered backprojection algorithm. (a) Forward projection. The left panel shows the boundaries of the original object (based on elliptical primitives) in our tomography workspace. The right panel shows the path integral of the object at an offset t along the projection axis. (b) Back projection. Non-filtered (left) and ρ-filtered (right) reconstructions of the original object with projections taken at every 1° interval from 0° to 180°. The boundaries of the original object are superimposed in white. There is excellent agreement between the reconstructed result and the source distribution, especially for filtered backprojection.

sions to our tomography setup. However, the optical design software Zemax is based on real units (mm) and, for consistency, we will adopt the tomography geometry as shown in Fig. 1. The complete 2-D workspace is a 10 mm × 10 mm square in which arbitrary objects can be placed at any point (as long as it does not intersect the entrance and exit ports). The transverse intercept of a ray at the exit port is given by t.

Note that the object under test is placed in free space, with an index $n = 1$. Hence we will subtract the free space reference of $n \cdot d = 10$ mm from all path length measurements.

2.B. Standard filtered backprojection algorithm

The backprojection algorithm for reconstructing the source distribution $f(x, y)$ from its projections is well established [1]. Fig. 2 demonstrates our implementation of the forward and filtered-back projection routines in Matlab. In Fig. 2(a), the standard geometry for computing straight line integrals is illustrated in the spatial workspace, and a particular projection along $\theta = 30°$ is shown. Fig. 2(b) shows the reconstructed geometry, using projections at every 1° interval from 0° to 180°. The left panel shows the naive, non-filtered backprojection result (for which we expect $1/r$ blur), while the

right panel shows the ρ-filtered backprojection result. The boundaries of the original source object is then superimposed. There is excellent agreement between the reconstructed distribution and the original source, as expected for the ideal problem of reconstruction from straight line projections.

2.C. Refracted forward-projections with Zemax

Having established the basic ρ-filtered backprojection algorithm, our next task is to compute forward projections of arbitrary objects with correct refraction. We make use of the ray tracing engine of Zemax, accessible from Matlab via the "MZDDE" toolbox [2].

Our Zemax model of the tomography setup is achieved by using the mixed sequential/non-sequential mode of the optical design software. As in Fig. 1, we define a 10 mm diameter "entrance port" surface, which acts as the optical stop for a 0°-collimated fan of rays that comprise the projection. These rays propagate towards the "exit port" surface where the optical path length is measured as a function of transverse position t at the exit port. (This arrangement models the experimental setup in which one can place a detector at any known position on the exit port, but has no *a priori* knowledge about the propagation path.) Between the two ports is a nonsequential object that contains an arbitrary source distribution under study. The targets in this paper were modeled in Creo Parametric (PTC Inc.) and imported into Zemax [3]. In the nonsequential mode of Zemax, rays can undergo arbitrarily complex interactions – including refraction, total internal reflection, polarization-dependent splitting (when enabled), and so on. Fig. 3 shows examples of refraction projections, which can be surprisingly complex even for simple objects. All objects have an index of $n_{\text{obj}} = 1.05$, *i.e.* 5% variation in index from the background. For the case of the circular and rectangular targets, Fig. 3 also shows, for comparison, the expected projection if the rays were nonrefracting.

There are two phenomena that are apparent in the projections of Fig. 3 which require special treatment.

2.C.1. Dark intervals at the exit port

First is the phenomenon of "dark intervals" at the exit port. When refraction is taken into account, uniform illumination at the entrance port does not guarantee complete illumination at the exit port. (In contrast, in the case of straight line projections, uniform exit port illumination is trivially guaranteed.) This phenomenon can be readily observed in the projection of a circular target (top row of Fig. 3), where the portion of the exit plane corresponding roughly to $1.5 < |t| < 2.5$ receives no rays. Dark intervals are problematic for our reconstruction algorithm since filtered backprojection is conceptually based on a convolution of the projection measurement with a ρ-weighted spatial kernel function.

For the purposes of filtered backprojection in this paper, I will apply, rather arbitrarily, cubic interpolation for the dark intervals in a given projection.

2.C.2. Multipath due to lensing

The second phenomenon that we must resolve is "multipath" or lensing of the rays. Consider the tilted square target in the second row of Fig. 3. Due to steep refraction and total internal reflection within the target, multiple rays can intercept the exit surface at the same height. This means that the optical path length as a function of exit coordinate t may be multiple-valued when refraction is taken into account. This is clearly a problem for the reconstruction routine, since our mathematical operations are not defined for multiple-valued functions.

When refraction is taken into account, the phenomenon of multipath is extremely common. Returning to the circular target of Fig. 3, one might naively expect that as the input ray approaches the top and bottom edges of the circle, the projected rays would monotonically fill the dark intervals noted in Section 2.C.1. In reality, the rays are refracted more steeply as they approach the edges of the circular target, which results in multipath in the interval $-1.5 < t < 1.5$.

Again, for the purposes of this paper, we will adopt a simple (but somewhat arbitrary) protocol for the resolution of multiple-valued projections. For any position t on the exit plane, we will take the minimum optical path length measurement as the single value of the projection that will be backprojected. Note that, in experimental practice, one might measure the propagation delay of a pulse from entry to exit port as a measure of the ray's optical path length. In such a protocol, the most obvious feature of the measurement is likely to be the minimum propagation delay among the various possible paths.

The last row of Fig. 3 illustrates how the phenomenon of dark intervals and multipath can create extremely complicated projection curves for even relatively simple targets (a tilted Stanford "S", which has just 22 facets).

3. Sample reconstruction problems

Now that we have discussed the immediate numerical issues posed by refraction, and our methods for their resolution, we show the results of filtered backprojection of the targets presented in Fig. 3. The numerical setup of the forward projection is as follows. For a fixed rotation from $\theta = 0°$ to 180° in 1° intervals, we:

1. Launch a fan of $N_{\text{rays}} = 5000$ rays at the entrance port; compute each ray's intercept t on the exit port as well as the ray's optical path length.
2. Bin the exit port intercept into $N_{\text{bins}} = 1000$ bins. Note that, if the rays were nonrefracting, there would be $N_{\text{rays}}/N_{\text{bins}} = 5$ rays per bin.
3. Find the minimum optical path length among the rays belonging a particular bin.
4. (Cubic) interpolate path length values for bins that received no rays.

By processing the refracted projection by the above protocol, we obtain a well-behaved function that is suitable for backprojection. See Fig. 4 for an example of

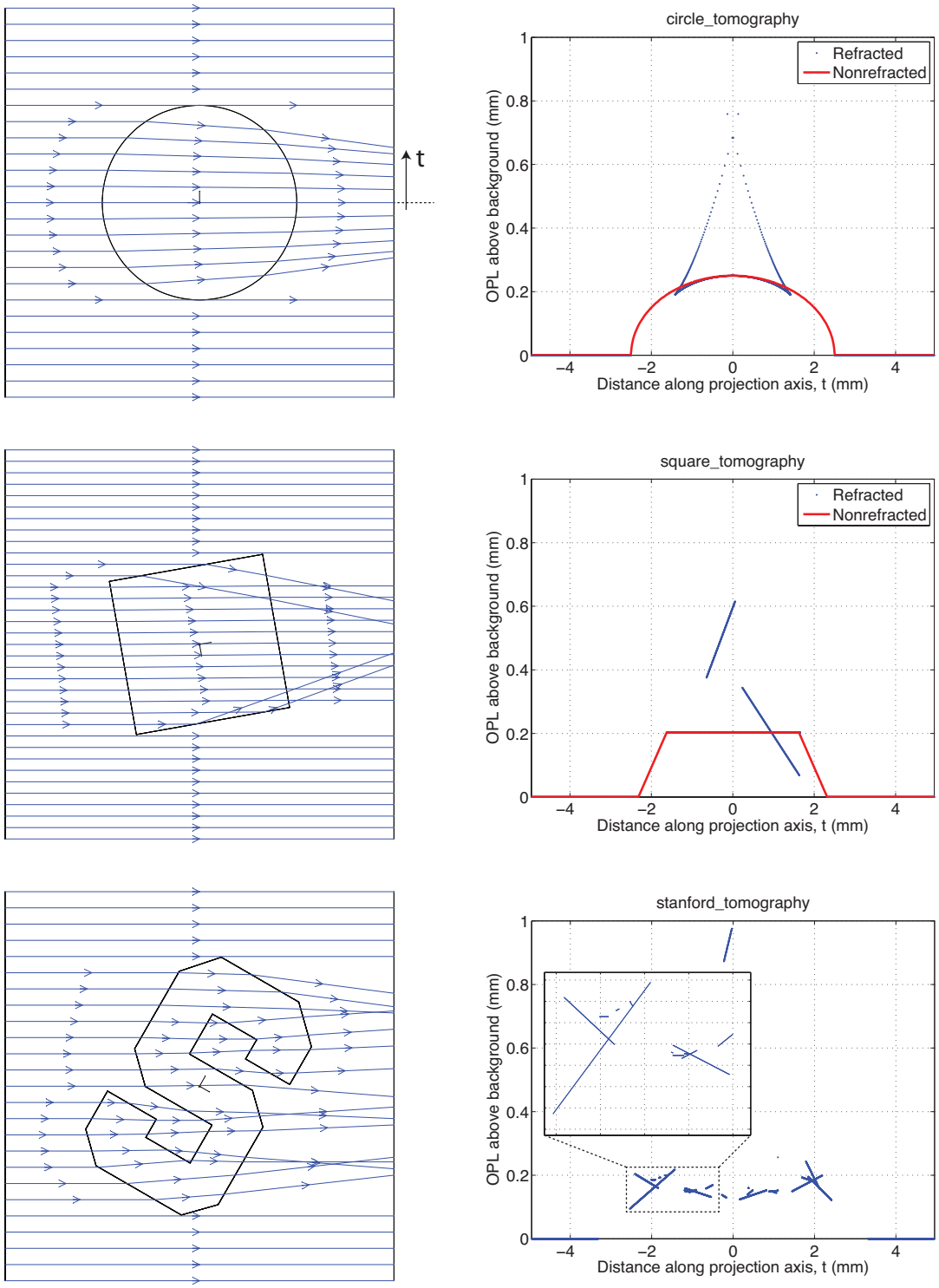

Fig. 3. Examples of refracted projection. All object indices are $n_{\text{obj}} = 1.05$. (Top row) A circle of diameter 5 mm. Note the phenomenon of "dark intervals" ($1.5 < |t| < 2.5$) at the exit surface, which are regions that receive no rays. (Middle row) A square of edge length 4 mm. Note the lensing of projection rays caused by refraction and total internal reflection. The optical path length as a function of exit surface intercept t can be multiple-valued. (Bottom row) Refraction through a tilted Stanford "S." Inset shows the level of complexity that can be observed in the path length projections, even with a relatively simple target. (The Stanford S logo has just 22 facets.)

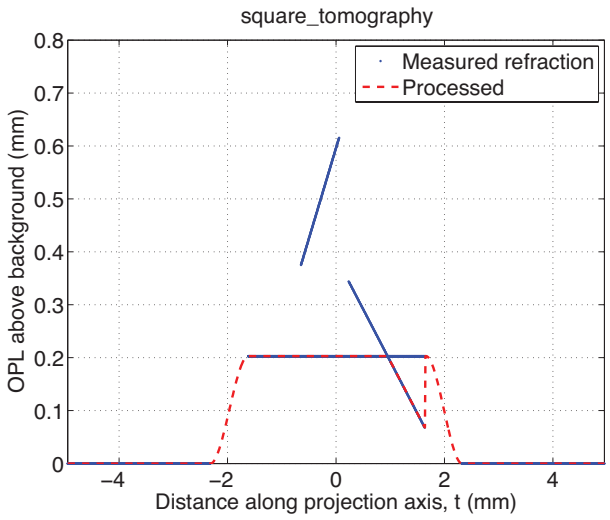

Fig. 4. Processing the raw refracted projection by the protocol described in Section 3. We take the minimum measured optical path length at each t, and interpolate the resulting values over the dark intervals.

the above protocol applied to the multi-valued projection through a tilted square (same source configuration as the second row of Fig. 3).

3.A. Circular target

The top row of Fig. 5 shows the backprojection reconstruction of the 5-mm diameter circle, with refraction taken into account in the forward model. For this simple target, we find that the general extent of the target can be recovered. However, the object boundary remains non-sharp even with ρ-filtered backprojection. The extent of the remaining blur is likely to be sensitive to the choice of interpolation method for the dark intervals. Note that our cubic interpolation for the dark intervals has a gentle taper at the edges of the object, while the "exact" nonrefracted projection will have a "hard" $\sqrt{1-t^2}$ dependence (*i.e.* slope not continuous at object boundary).

3.B. Square target

More interesting is the backprojection reconstruction of the 4-mm wide square target, shown in the middle row of Fig. 5. In both naive and filtered backprojections, we find that the object does not appear symmetric about the $x = 0$ plane. This is reasonable, since symmetry about $x = 0$ for the ray paths is broken when refraction is taken into consideration. In turn, this implies that when refraction is taken into account a full 360° rotation of the target will yield more information than just the 0° to 180° scan.

Note that the edges of the square in the ρ-filtered reconstruction appear sharper than their counterparts in the reconstruction of the circle. This is intuitively plausible since ideal (nonrefracting) projections of the square will yield linear tapers at the edges, which are well approximated by our cubic interpolation as shown in Fig. 4. (Compare to the nonrefracting projection in the second row of Fig. 3.) We are led to the general idea that different interpolation schemes may be well suited for different classes of source objects.

3.C. Stanford "S"

The bottom row of Fig. 5 shows the failed reconstruction of the Stanford "S." The original source is entirely unrecognizable, especially in the ρ-filtered result which appears to be nearly uniform intensity over the workspace. The abysmal reconstruction strongly suggests that the backprojection algorithm is inadequate for even modestly complicated refracting targets.

4. Further work

We have shown that it is possible to utilize a commercial ray-tracing engine to model ray-based tomography systems with correct refraction (and reflection) behavior. We have shown that the backprojection algorithm fails for even modestly complicated refracting targets, such as the Stanford "S" with its 22 facets. There are many further ideas to pursue.

First, we may try additional targets. If the circular target is permissible, while the Stanford "S" is not, it would be interesting to evaluate the "reconstructability" of refracting targets as a function of their shape complexity. (It may be possible to characterize the complexity of a refracting target, for example, by the RMS deviation of the refracting ray intercepts from their nonrefracting intercepts.) Similarly, we may investigate the reconstructability of a fixed shape as a function of varying index. Finally, it would also be interesting to examine non-simple targets, *i.e.* objects with internal structure such as the elongated ellipse in Fig. 2.

Second, the two-dimensional workspace considered in this paper should be generalized into three dimensions. This is necessary since a ray intersecting an arbitrary object in the workspace may refract not only within the plane, but possibly also out of plane! When refraction is taken into account, the simple idea of taking a planar "slice" of a complex object is in general not valid.

Finally, given the abysmal performance of the filtered backprojection method for refracted projection measurements, we are left wanting for better reconstruction algorithms!

References

[1] Kak, A. C. and Slaney, Malcolm. *Principles of Computerized Tomographic Imaging*, IEEE Press, 1988.
[2] Griffith, D. *How to talk to Zemax from MATLAB*, Zemax Knowledge Base.
[3] Nicholson, M. *How to import CAD objects*, Zemax Knowledge Base.

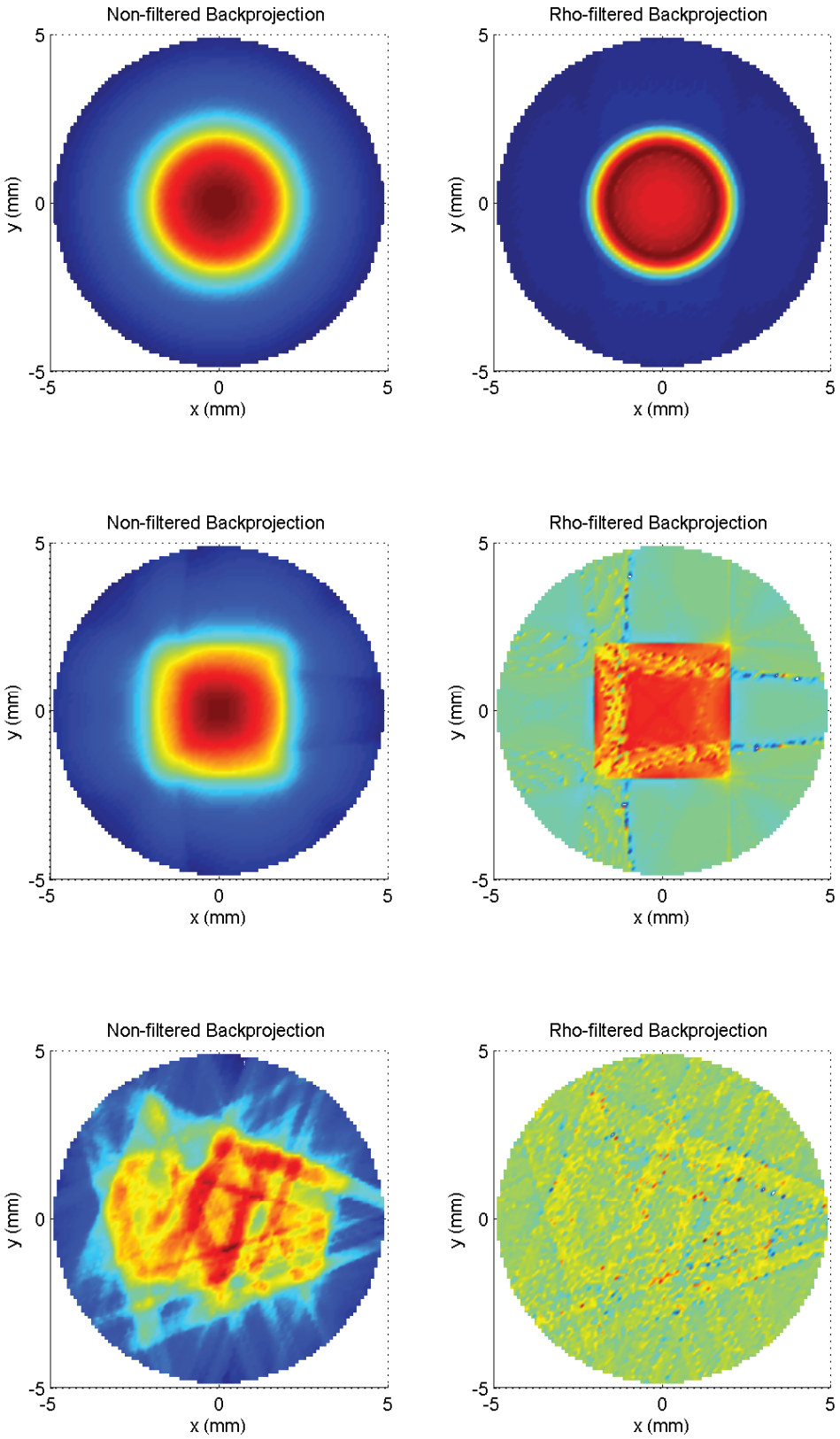

Fig. 5. Examples of refracted backprojection, using projections at every 1° interval from 0° to 180°. All object indices are $n_{\text{obj}} = 1.05$. (Top row) A circle of diameter 5 mm. Note that the object boundaries are not sharp, even under the ρ-filter. (Middle row) A square of edge length 4 mm. Symmetry about $x = 0$ is broken when refraction is taken into acount. (Bottom row) Failed reconstruction of the Stanford "S." The original source is entirely unrecognizable. In particular, the ρ-filtered result gives almost no information about the source.